J. Plasma Physics (2013), vol. 79, part 3, pp. 257–265. © Cambridge University Press 2012
doi:10.1017/S0022377812000918

Nonlinear translational symmetric equilibria relevant to the L–H transition

Ap. KUIROUKIDIS[1] and G. N. THROUMOULOPOULOS[2]

[1]Technological Education Institute of Serres, 62124 Serres, Greece
[2]Department of Physics, University of Ioannina, Association Euratom-Hellenic Republic, 45110 Ioannina, Greece
(gthroum@uoi.gr)

(Received 13 July 2012; revised 27 August 2012; accepted 17 September 2012; first published online 12 November 2012)

Abstract. Nonlinear z-independent solutions to a generalized Grad–Shafranov equation (GSE) with up to quartic flux terms in the free functions and incompressible plasma flow non-parallel to the magnetic field are constructed quasi-analytically. Through an ansatz, the GSE is transformed to a set of three ordinary differential equations and a constraint for three functions of the coordinate x, in Cartesian coordinates (x, y), which then are solved numerically. Equilibrium configurations for certain values of the integration constants are displayed. Examination of their characteristics in connection with the impact of nonlinearity and sheared flow indicates that these equilibria are consistent with the L–H transition phenomenology. For flows parallel to the magnetic field, one equilibrium corresponding to the H state is potentially stable in the sense that a sufficient condition for linear stability is satisfied in an appreciable part of the plasma while another solution corresponding to the L state does not satisfy the condition. The results indicate that the sheared flow in conjunction with the equilibrium nonlinearity plays a stabilizing role.

1. Introduction

For axisymmetric toroidal plasma equilibria, the force–balance equation and Maxwell's equations reduce to the Grad–Shafranov equation (GSE) for the poloidal magnetic flux function ψ (Grad and Rubin 1958; Shafranov 1958). Analytical solutions to the GSE are obtained by specifying the plasma pressure and poloidal current functions of ψ, usually in such a way as to linearize the resulting partial differential equation (e.g. Solovév 1968; Herrnegger 1972; Maschke 1972; Berk et al. 1981; Mc Carthy 1999; Weening 2000; Yavorskij et al. 2001; Atanasiu et al. 2004; Cerfon and Freidberg 2010; Srinivasan et al. 2010). Analytical solutions to the GSE are very useful for theoretical studies of plasma equilibrium, stability and transport as well as benchmarks for numerical codes (Mukhopadhyay 2000). Also, it has been established in a variety of magnetic configurations that sheared flows can reduce turbulence and produce transport barriers, which under certain conditions can extend to the whole plasma (e.g. Terry 2000). In view of a fusion reactor, the spontaneous formation of transport barriers, i.e. those driven by internal processes even in the absence of external sources, is of particular interest. For this reason among others, stationary equilibria with plasma flow have been extensively studied on the basis of generalized GSEs (e.g. Mashke and Perrin 1984; Clemente and Farengo 1984; Greene 1988; Throumoulopoulos and Pantis 1996; Throumoulopoulos and Tasso 1997, 2010, 2012; Goedbloed and Lifschitz 1997; Tasso and Throumoulopoulos 1998; Betti and Freidberg 2000; Simintzis et al. 2001; Krasheninnikov et al. 2002; Poulipoulis et al. 2005; Throumoulopoulos et al. 2006, 2008, 2009; Apostolaki et al. 2008; Khater and Moawad 2009; Kuiroukidis 2010; Kuiroukidis and Throumoulopoulos 2011, 2012; Tsui et al. 2011; Shi 2011). In particular, although complex numerical codes are extensively used to attempt simulations of the L–H transition, certain equilibrium considerations in connection with this transition are helpful (e.g. Ilgisonis and Pozdnyakov 2004; Solano 2004; Garcia and Giruzzi 2010; Tsui and Navia 2012).

The simplest known and widely used in various studies, analytical solution to the GSE, is the Solovév equilibrium (Solovév 1968). Extension of the original Solovév solution, to include the possibility of sheared flows appeared in Simintzis et al. (2001). In other extensions additional free parameters were introduced to construct configurations with fusion relevant plasma boundaries and desirable values of confinement figures of merit as the safety factor on magnetic axis (Cerfon and Freidberg 2010; Srinivasan et al. 2010; Throumoulopoulos and Tasso 2012). Most of the solutions are associated with pressure and current profiles, including up to quadratic terms in the flux function ψ to linearize the resulting equation (Solovév 1968; Herrnegger 1972; Maschke 1972; Berk et al. 1981; Mc Carthy 1999; Weening 2000; Yavorskij et al. 2001; Atanasiu et al. 2004; Cerfon and Freidberg 2010; Srinivasan et al. 2010). Linear equilibria with flow were constructed in (Clemente and Farengo 1984; Mashke and Perrin 1984; Greene 1988;

Throumoulopoulos and Pantis 1996; Goedbloed and Lifschitz 1997; Throumoulopoulos and Tasso 1997, 2012; Tasso and Throumoulopoulos 1998; Betti and Freidberg 2000; Simintzis et al. 2001; Krasheninnikov et al. 2002; Poulipoulis et al. 2005; Throumoulopoulos et al. 2006, 2008; Apostolaki et al. 2008; Khater and Moawad 2009; Kuiroukidis 2010; Kuiroukidis and Throumoulopoulos 2011, 2012; Tsui et al. 2011; Shi 2011,and references cited therein). Also, the nonlinear translational symmetric equilibria of 'cat eyes' and counter-rotating vortices with flow parallel to the magnetic field were studied in Throumoulopoulos et al. (2009) and Throumoulopoulos and Tasso (2010). These nonlinear equilibria, however, are periodic in one direction (x) and therefore the plasma is not bounded along this direction.

In most of the above cases, the axisymmetric equilibria are obtained as separable solutions of GSE. A novel non-separable class of solutions was found in Kuiroukidis (2010) describing up-down symmetric configurations with incompressible flows parallel to the magnetic field and it was extended recently to include asymmetric configurations (Kuiroukidis and Throumoulopoulos 2011) and flows of arbitrary direction (Kuiroukidis and Throumoulopoulos 2012). For non-parallel flows, the question of the stability is usually not considered and this is partly due to the difficulty of the subject and the absence of a concise criterion. Few sufficient conditions for linear stability are available only for parallel flows (Friedlander and Vishik 1995; Vladimirov and Ilin 1998; Throumoulopoulos and Tasso 2007). In previous studies, we found that the stability condition of Throumoulopoulos and Tasso (2007) is not satisfied for the linear equilibria of Apostolaki et al. (2008) and Throumoulopoulos and Tasso (2012) while it is satisfied within an appreciable part of the plasma for the nonlinear equilibria of Throumoulopoulos et al. (2009) and Throumoulopoulos and Tasso (2010). This led us to the conjecture that the equilibrium nonlinearity may act synergetically with the sheared flow to stabilize the plasma.

The aim of the present study is to construct certain two-dimensional nonlinear up-down symmetric equilibria with incompressible flow of arbitrary direction in z-independent geometry. They are more pertinent to a magnetically confined plasma than those of Throumoulopoulos et al. (2009) and Throumoulopoulos and Tasso (2010) because the plasma is bounded on the poloidal plane. Another reason for considering translational symmetry is the many free physical and geometrical parameters involved in connection with the flow amplitude, direction and shear, equilibrium nonlinearity, symmetry and toroidicity. Thus, in the presence of nonlinearity, one first could exclude toroidicity. The study is performed quasi-analytically through a non-separable ansatz under which the GSE is transformed to a set of three ordinary differential equations and a constraint for three functions. The solutions give nested magnetic surfaces and their characteristics are studied by means of certain equilibrium quantities and confinement figures of merit as the safety factor, electric field and $\mathbf{E}\times\mathbf{B}$ velocity shear. Also, for parallel flows the linear stability is considered by means of the aforementioned sufficient condition (Throumoulopoulos and Tasso 2007). The results are in qualitative agreement with phenomenological characteristics of an edge transport barrier, confirm relevant scenarios (Terry 2000; Simintzis et al. 2001) and support the above conjecture.

The organization of the paper is as follows. In the first section, we briefly review the general setting for the equations of incompressible flow with translational symmetry together with the generalized GSE. In Sec. 2, the proposed ansatz and the resulting equations are presented, which then are integrated numerically. In Sec. 3, we consider the solutions for certain values of the various parameters and integration constants and discuss the most important equilibrium properties. In Sec. 4, the criterion for linear stability is applied to the equilibria constructed for parallel flows. Section 5 summarizes the study and briefly proposes potential extensions.

2. Translational symmetric equilibria with flow

The equilibrium of a cylindrical plasma with incompressible flow and arbitrary cross-sectional shape satisfies the equation (Throumoulopoulos and Tasso 1997; Simintzis et al. 2001)

$$\left(1-M_p^2\right)\nabla^2\psi-\frac{1}{2}\left(M_p^2\right)'|\nabla\psi|^2+\frac{d}{d\psi}\left(\mu_0 P_s+\frac{B_z^2}{2}\right)=0 \tag{1}$$

for the poloidal magnetic flux function ψ. Here, $M_p(\psi)$, $P_s(\psi)$, $\rho(\psi)$ and $B_z(\psi)$ are respectively the poloidal Alfvén Mach function, pressure in the absence of flow, density and magnetic field parallel to the symmetry axis z, which are surface quantities. Because of the symmetry, the equilibrium quantities are z-independent and the axial velocity v_z does not appear explicitly in (1). Derivation of (1) is based on the following two steps. First, express the divergence-free fields in terms of scalar quantities as

$$\mathbf{B}=B_z\nabla z+\nabla z\times\nabla\psi,$$

$$\mu_0\mathbf{j}=\nabla^2\psi\nabla z-\nabla z\times\nabla B_z,$$

$$\rho\mathbf{v}=\rho v_z\nabla z+\nabla z\times\nabla F,$$

and the electric field by $\mathbf{E}=-\nabla\Phi$. Second, project the momentum equation, $\rho(\mathbf{v}\cdot\nabla)\mathbf{v}=\mathbf{j}\times\mathbf{B}-\nabla P$, and Ohm's law, $\mathbf{E}+\mathbf{v}\times\mathbf{B}=0$, along the symmetry direction z, $\mathbf{B}$ and $\nabla\psi$. The projections yield four first integrals in the form of surface quantities (two out of which are $F(\psi)$ and $\Phi(\psi)$), Eq. (1) and the Bernoulli relation for the

https://doi.org/10.1017/S0022377812000918 Published online by Cambridge University Press

pressure

$$P = P_s(\psi) - \frac{1}{2\mu_0} M_p^2(\psi)|\nabla\psi|^2. \tag{2}$$

Because of the flow, P is not a surface quantity. Also, the density becomes surface quantity because of incompressibility and $M_p^2(\psi) = (F'(\psi))^2/(\mu_0\rho)$. Five of the surface quantities, chosen here to be P_s, ρ, B_z, M_p^2 and v_z, remain arbitrary.

Using the transformation

$$u(\psi) = \int_0^{\psi} \left[1 - M_p^2(g)\right]^{1/2} dg, \quad \left(M_p^2 < 1\right), \tag{3}$$

Equation (1) is transformed to

$$\nabla^2 u + \frac{d}{du}\left(\mu_0 P_s + \frac{B_z^2}{2}\right) = 0. \tag{4}$$

Note that transformation (3) does not affect the magnetic surfaces, it just relabels them. Equation (4) is identical in form with the static equilibrium equation. In the present study, we assign the free-function term in (4) as

$$\left(\mu_0 P_s + \frac{B_z^2}{2}\right) = c_0 + c_1 u + c_2\frac{u^2}{2} + c_3\frac{u^3}{3} + c_4\frac{u^4}{4}, \tag{5}$$

where $c_0, c_1, \ldots, c_4$ are free parameters.

3. Proposed ansatz

We use (5) into (4), employ the ansatz

$$u = \frac{N_1(x)y^2 + f(x)D_0(x)}{y^2 + D_0(x)}, \tag{6}$$

and equate the nominator of the resulting equation to zero. From the y^6 terms, we obtain (a prime denotes derivative with respect to x)

$$N_1'' + c_1 + c_2 N_1 + c_3 N_1^2 + c_4 N_1^3 = 0. \tag{7}$$

From the y^0 terms, we obtain the constraint $C_s = 0$, where

$$C_s = 2(N_1 - f) + D_0[c_1 + c_2 f + c_3 f^2 + c_4 f^3]\,(= 0). \tag{8}$$

The y^4 and y^2 terms, after rearrangement, yield

$$f'' + 2(N_1 - f)\left(\frac{D_0'}{D_0}\right)^2 - \frac{8(N_1 - f)}{D_0} + c_4(N_1 - f)^3 = 0 \tag{9}$$

and

$$D_0'' + 2\frac{(N_1' - f')}{(N_1 - f)}D_0' + 2\frac{(D_0')^2}{D_0} - 6 + c_3 D_0(N_1 - f) + 3c_4 D_0 N_1(N_1 - f) = 0. \tag{10}$$

Equation (7) is solved using the tanh method (Malfliet 2004), a method of solving nonlinear differential equations, which was also employed in Khater and Moawad (2009). We have two solutions. The first is $N_1(x) = a_0 + a_1 \tanh(vx)$, where

$$\begin{aligned} c_1 + c_2 a_0 + c_3 a_0^2 + c_4 a_0^3 &= 0, \\ c_2 + c_3(2a_0) + c_4(3a_0^2) &= 2v^2, \\ c_3 + c_4(3a_0) &= 0, \\ c_4\left(a_1^2\right) &= -2v^2, \end{aligned} \tag{11}$$

and the second is $N_1(x) = a_0 + a_1/\cosh(vx)$, where

$$\begin{aligned} c_1 + c_2 a_0 + c_3 a_0^2 + c_4 a_0^3 &= 0, \\ c_2 + c_3(2a_0) + c_4\left(3a_0^2\right) &= -v^2, \\ c_3 + c_4(3a_0) &= 0, \\ c_4\left(a_1^2\right) &= 2v^2. \end{aligned} \tag{12}$$

4. Solutions and equilibrium properties

We have solved numerically (8)–(10). Using the first of the solutions for N_1, namely the tanh solution, we obtained the equilibrium of Fig. 1. We have used $a_0 = 1.1$, $a_1 = 2.5$, $v = 0.6$ and in (5) $c_0 = 2.588$, $c_1 = -0.638$, $c_2 = 0.302$, $c_3 = 0.38$, $c_4 = -0.115$. The boundary flux surface corresponds to $u_b = 0.11$ while on the magnetic axis $u_a = 0$. The constraint was kept close to zero for the whole of the integration process and we got an average value of $|C_s|$ equal to 0.10. Given the nonlinearity and complexity of the method, this implies that the solution is indeed acceptable. Simple quadratic fitting

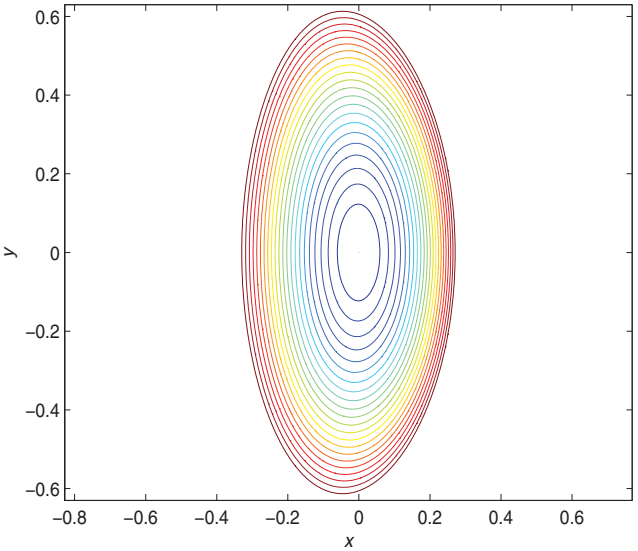

Figure 1. (Colour online) Equilibrium 1. The bounding flux surface corresponds to $u_b = 0.11$, with $u_a = 0$, for the magnetic axis. For this equilibrium the average value of $|C_s|$ is 0.10.

https://doi.org/10.1017/S0022377812000918 Published online by Cambridge University Press

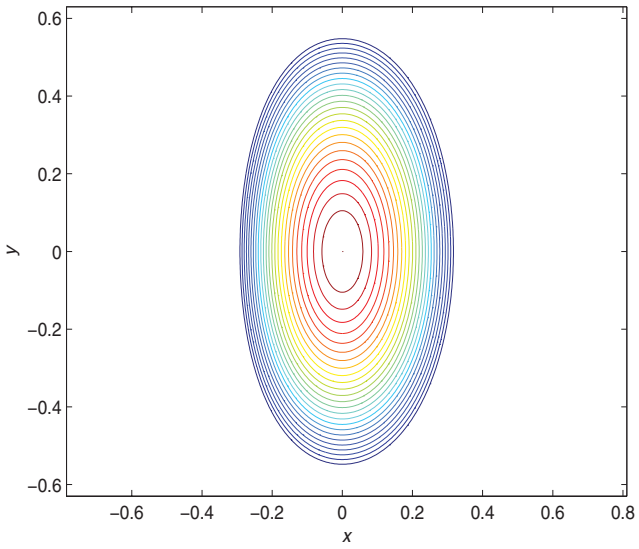

Figure 2. (Colour online) Equilibrium 2. The bounding flux surface corresponds to $u_b = -0.05$, with $u_a = 0$, for the magnetic axis. For this equilibrium the average value of $|C_s|$ is 0.10.

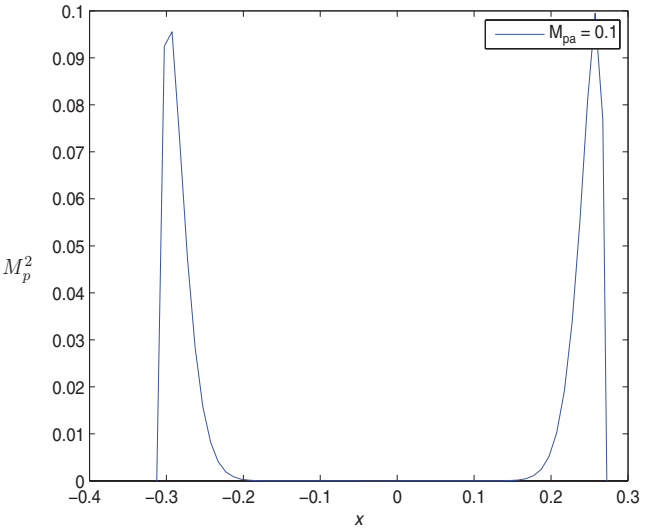

Figure 3. (Colour online) L–H transition-like Mach function in connection with (13) with $n = 1$ and a maximum localized at a distance from the boundary as large as one-tenth of the minor radius.

gives

$$f = 1.272x^2 + 0.049x + 0.001 \text{ and } D_0 = 1.488x + 3.3.$$

Using the second of the solutions for N_1, namely the cosh solution, we obtained the equilibrium of Fig. 2. We have used $a_0 = 1.0$, $a_1 = -1.6$, $v = 1.15$ and in (5) $c_0 = 2.588$, $c_1 = 0.289$, $c_2 = 1.777$, $c_3 = -3.099$, $c_4 = 1.033$. The boundary flux surface corresponds to $u_b = -0.05$ while on the magnetic axis $u_a = 0$. The constraint was kept close to zero for the whole of the integration process and the average value of $|C_s|$ was 0.10. Simple quadratic fitting gives

$$f = -0.542x^2 + 0.009x \text{ and } D_0 = 0.994x^2 + 3.3.$$

Here instead of the velocity v_z we have used the axial Mach function, $M_z^2(u) = v_z^2/(B_z^2/(\mu_0\rho))$, and the approximation $M_z^2 \approx M_p^2 = (F')^2/(\mu_0\rho)$ in relation to the tokamak scaling $B_p \approx 0.1B_z$ and $v_p \approx 0.1v_z$. In addition, to completely construct the equilibrium we have made the following choices:

$$M_p^2 = C_p(u - u_b)^n(u_a - u)^m, \tag{13}$$

$$C_p = M_{pa}\left[\frac{m(u_a - u_b)}{m+n}\right]^{-m}\left[\frac{n(u_a - u_b)}{m+n}\right]^{-n},$$

$$M_z^2 = C_z(u - u_b)^n(u_a - u)^m, \tag{14}$$

$$C_z = M_{za}\left[\frac{m(u_a - u_b)}{m+n}\right]^{-m}\left[\frac{n(u_a - u_b)}{m+n}\right]^{-n},$$

$$B_z^2 = B_{z0}^2\left[1 - \gamma\left(1 - \frac{u}{u_b}\right)\right], \tag{15}$$

$$\rho = \rho_a\left(1 - \frac{u}{u_b}\right)^{\lambda}, \tag{16}$$

for the poloidal Mach function, axial Mach function, axial magnetic field and density, respectively, with $B_{z0} =$

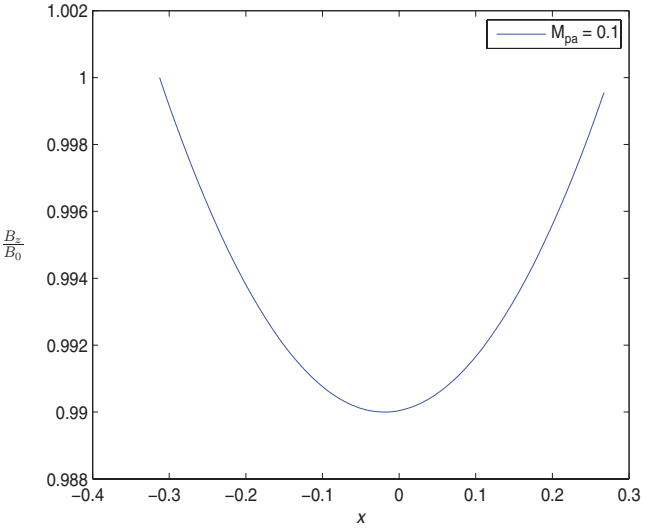

Figure 4. (Colour online) Typical diamagnetic axial magnetic field profile normalized with respect to the value at the magnetic axis in connection with (15).

2.24 T, $\rho_a = 4 \times 10^{-7}$ Kgr m^{-3}, $\gamma = 0.02$, $u_a = 0$, $u_b = 0.11$ W m^2 (with the subscripts a and b indicating the magnetic axis and boundary, respectively), $\lambda = 0.5$, $m = 9n$ and $M_{za} = 1.1M_{pa}$ with various values of the parameters M_{pa} and n. Here, (13) and (14) can describe Mach functions localized in the edge plasma region in connection with the L–H transition (in particular, flows localized nearly in one-tenth of the exterior plasma will be considered as shown in Fig. 3); (15) represents a diamagnetic $B_z(u)$ (Fig. 4). Then, (2) and (5) imply a pressure peaked on axis (Fig. 5).

Furthermore, we have examined certain equilibrium characteristics by means of the safety factor, magnetic shear, axial current density, radial electric field and $\mathbf{E}\times\mathbf{B}$ velocity shear, and found the following results.

https://doi.org/10.1017/S0022377812000918 Published online by Cambridge University Press

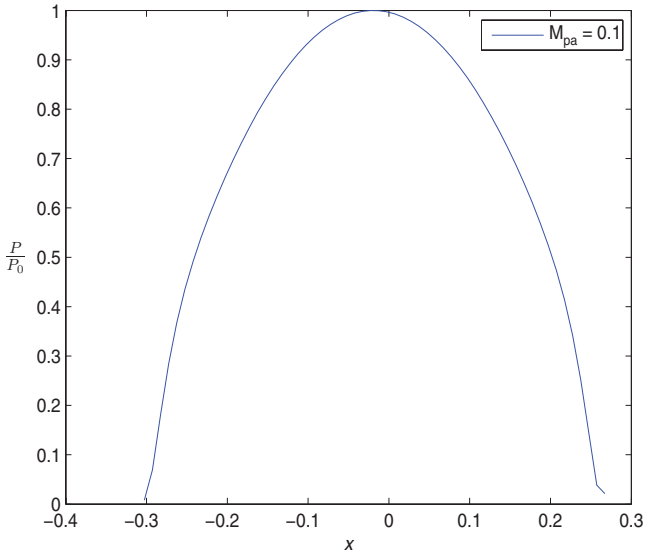

Figure 5. (Colour online) Pressure profile at $y = 0$ for Equilibrium 1 with $P_0 = 1.6 \times 10^5$ Pa.

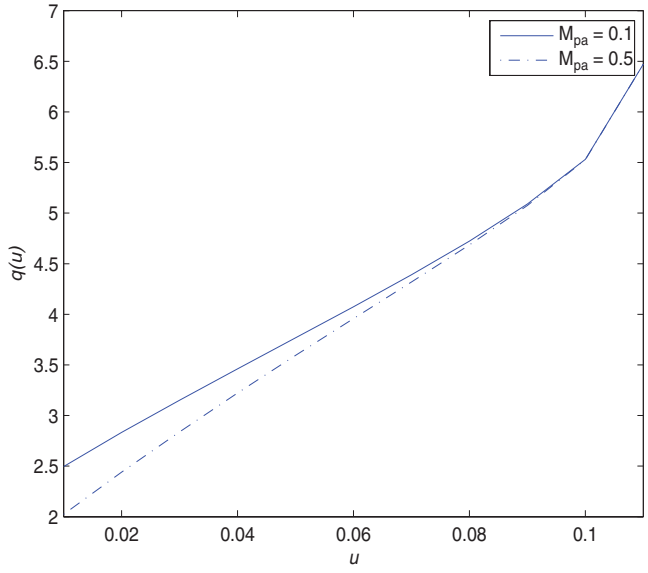

Figure 6. (Colour online) Safety factor for the solution of Equilibrium 1.

1. The safety factor for both solutions shown in Figs 6 and 7 is slightly affected by the flow. Also, the flow slightly affects the magnetic shear given by $s(u) = 2(V/q)(dq/dV)$, as can be seen in Fig. 8 for Equilibrium 1. A similar plot holds for Equilibrium 2.
2. The radial electric field for the two solutions has an extremum in the edge region which increases with the flow (Figs 9 and 10). The position of the extremum, however, is nearly unaffected by the flow. These characteristics are indicative that the solutions may be relevant to the L–H transition as discussed in Simintzis et al. (2001), where a similar behavior of the electric field was found (Fig. 3 therein).
3. The $\mathbf{E} \times \mathbf{B}$ velocity shear, which is believed to play a role in the transitions to improved confinement

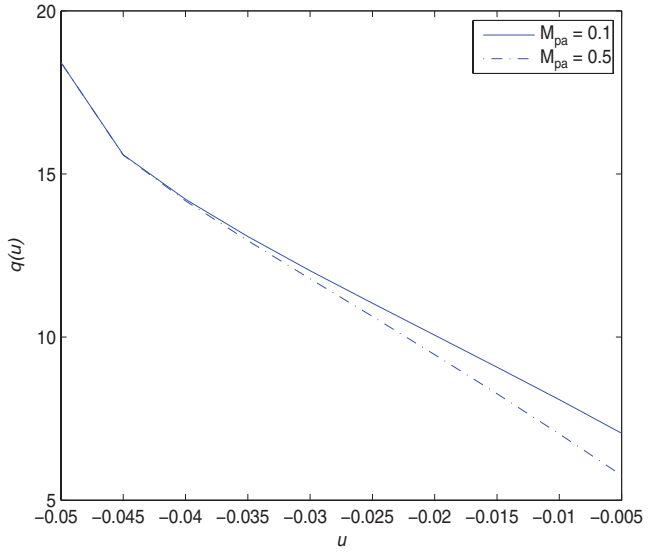

Figure 7. (Colour online) Safety factor for the solution of Equilibrium 2. Note that the outer boundary surface corresponds to $u = -0.05$ while the magnetic axis to $u = -0.005$.

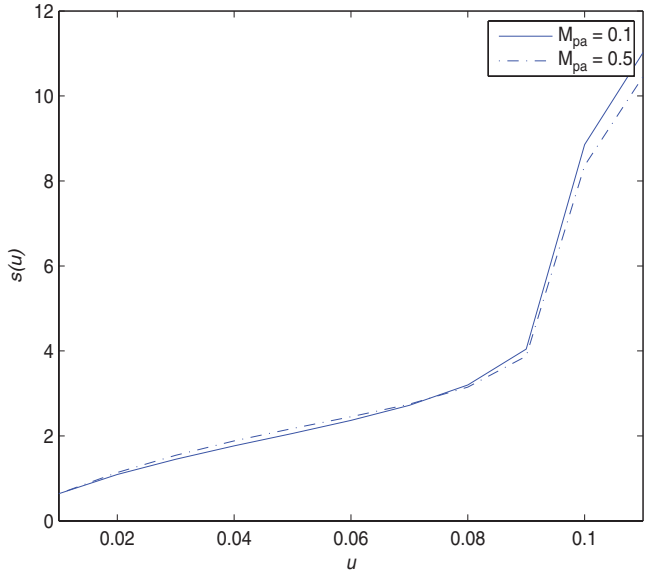

Figure 8. (Colour online) Magnetic shear for the solution of Equilibrium 1. It is slightly affected by the presence of the flow. A similar plot holds for Equilibrium 2.

regimes of magnetically confined plasmas, is given by

$$\omega_{E\times B} = \left| \frac{d}{dr} \left[\frac{\mathbf{E} \times \mathbf{B}}{B^2} \right] \right|, \tag{17}$$

where r is the length variable normal to the magnetic surfaces. For Equilibrium 1 it is plotted in Fig. 11; a similar plot holds for Equilibrium 2. Here, $\omega_{E\times B}$ is increased by the flow in the edge region outer from the local minimum while it remains nearly unaffected in the central region. This is another indication supporting the relevance of the solutions to the L–H transition.

https://doi.org/10.1017/S0022377812000918 Published online by Cambridge University Press

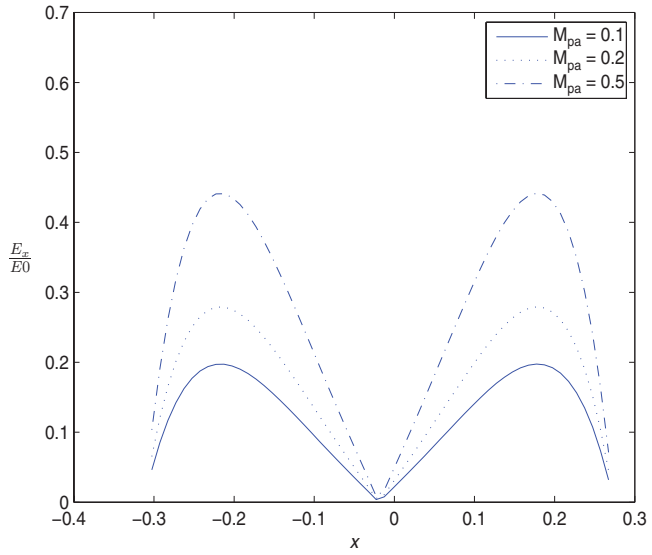

Figure 9. (Colour online) Normalized electric field with respect to $E_0 = 280$ kV m^{-1} for the solution of Equilibrium 1. The extremum of the electric field increases with flow; the position of the extremum however is not significantly affected by it.

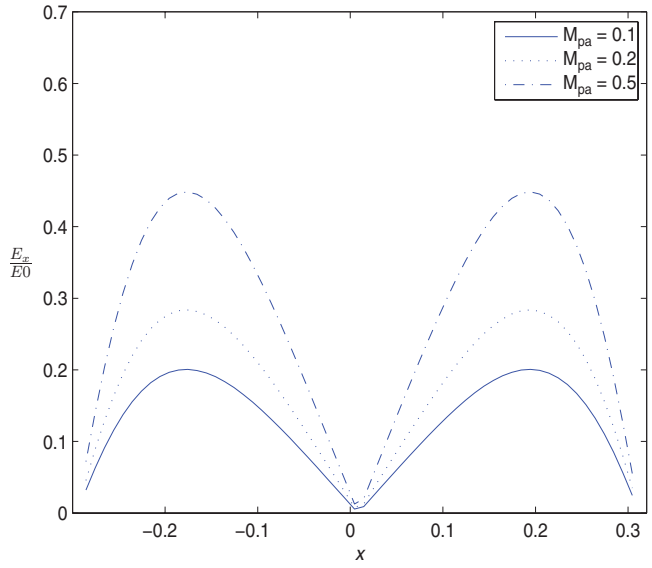

Figure 10. (Colour online) Electric field for the solution of Equilibrium 2. The extremum of the electric field increases with flow; the position of the extremum however is not significantly affected by it.

4. The flow makes the axial ('toroidal') current density profile hollow as shown in Fig. 12 for Equilibrium 1. (A similar $j_{\rm tor}$ profile is found for Equilibrium 2.) The larger the flow the stronger is the hollowness. Hollow $j_{\rm tor}$ profiles are usually related to the formation of internal transport barriers in tokamaks. However, in spite of this characteristic and the fact that $\omega_{E\times B}$ becomes maximum on the magnetic axis (Fig. 11), it is unlikely that the present equilibria are related to internal transport barriers because the safety factor is monotonically increasing from the magnetic axis to the plasma edge (Figs 6 and 7). According to observations in tokamaks, e.g. de Vries et al. (2009) for Joint European Torus (JET) and Shafer et al. (2009) for Doublet III-D tokamak (D III-D), it is the reversed magnetic shear that plays a role in triggering the Internal Transport Barrier's (ITB) development. Also, as can be seen in Figs 6 and 7, the flow makes the central q values lower.

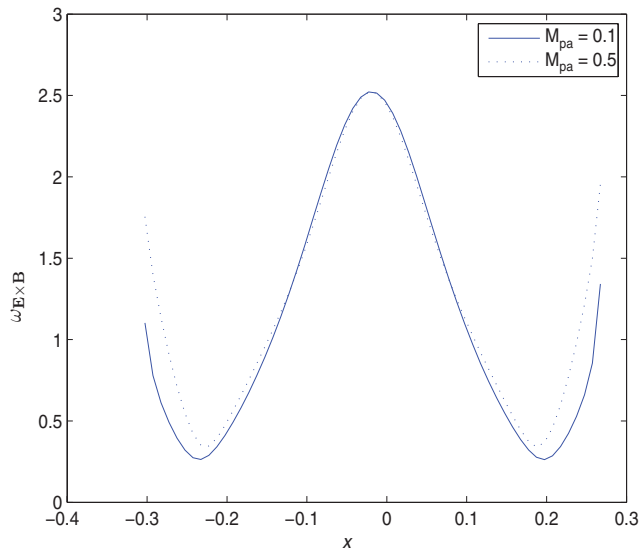

Figure 11. (Colour online) The $\mathbf{E}\times\mathbf{B}$ velocity shear, for the solution of Equilibrium 1. It increases slightly with the presence of flow in the edge region. A similar plot holds for Equilibrium 2.

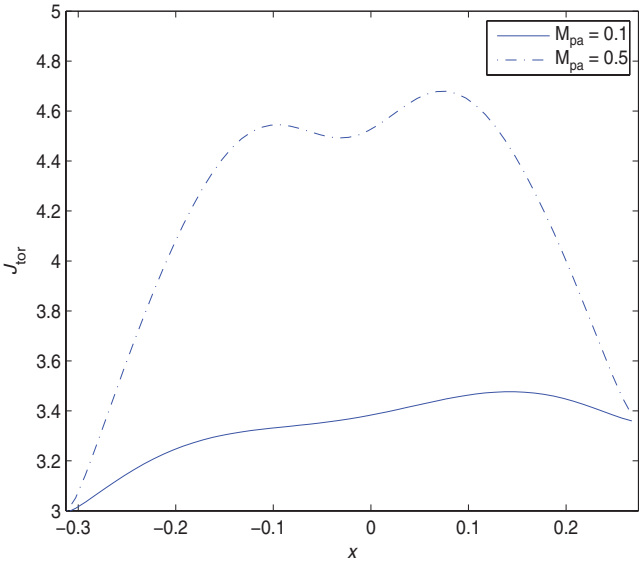

Figure 12. (Colour online) Axial current density in MA as a function of the flow parameter M_{pa}, for the solution of Equilibrium 1. As the flow increases, a hollow profile in the core of the equilibrium appears and it becomes larger for larger values of the flow.

5. Stability consideration

We now consider the important issue of the stability of the solutions constructed in Sec. 4 with respect to small linear magnetohydrodynamic perturbations by applying the sufficient condition of Throumoulopoulos and Tasso (2007). This condition states that a general steady state

https://doi.org/10.1017/S0022377812000918 Published online by Cambridge University Press

of a plasma of constant density and incompressible flow parallel to $\mathbf{B}$ is linearly stable to small three-dimensional perturbations if the flow is sub-Alfvénic ($M^2 < 1$) and $A \geqslant 0$, where A is given below by (18). Consequently, using henceforth dimensionless quantities, we set $\rho = 1$. Also, for parallel flows ($\mathbf{v} = M\mathbf{B}$), it holds $M_p \equiv M_z \equiv M$. In fact, if the density is uniform at equilibrium, it remains so at the perturbed state because of incompressibility (Tasso and Throumoulopoulos 2012). In the u space for axisymmetric equilibria, A assumes the form

$$A = -\bar{g}^2 \left[(\mathbf{j} \times \nabla u) \cdot (\mathbf{B} \cdot \nabla)\nabla u + \left(\frac{M_p^2}{2}\right)' \frac{|\nabla u|^2}{\left(1 - M_p^2\right)^{3/2}} \left\{ \nabla u \cdot \nabla (B^2/2) + \bar{g} \frac{|\nabla u|^2}{\left(1 - M_p^2\right)^{1/2}} \right\} \right] \tag{18}$$

with

$$\bar{g} := \frac{P_s'(u) - \left(M_p^2\right)' B^2/2}{1 - M_p^2}.$$

The symbolic computation of A over a wide rage of parametric values led to the following results:

1. Equilibrium 1 is not satisfied, since $A < 0$ everywhere, while Equilibrium 2 is satisfied in an appreciable part of the plasma region. However, it is noted that since the stability condition is necessary, $A < 0$ does not imply that an equilibrium is unstable. An example of the sign of A for Equilibrium 2 is given in the three-dimensional plot of Fig. 13. Also, profiles of A in the middle-plane $y = 0$ for a static and a stationary equilibrium are shown in Fig. 14.
2. Increase of M_{pa} makes A more positive in the edge region as can be seen in the example of Fig. 14. A similar impact on A has the flow shear parameter n (13), as can be seen in Fig. 15, showing the profile of $\delta A = A(y = 0, n = 2) - A(y = 0, n = 1)$.
3. The equilibrium nonlinearity in connection with the parameters c_3 and c_4 has a stabilizing effect in the edge region as shown in the example of Fig. 16, which plots the profile of the difference δA between a nonlinear and a linear Equilibrium 2.

According to the above results and the belief that the sheared flow is developed during the L–H transition, we conjecture that a static Equilibrium 1 could correspond to the L state and a stationary Equilibrium 2 with $\mathbf{E} \times \mathbf{B}/B^2$ velocity shear to the H state. In a quasi-static evolution approximation, the plasma could then evolve through successive states with increased sheared flow (increasing values of the parameters M_{pa} and M_{za} and most importantly increasing values of the shearing parameters m and n).

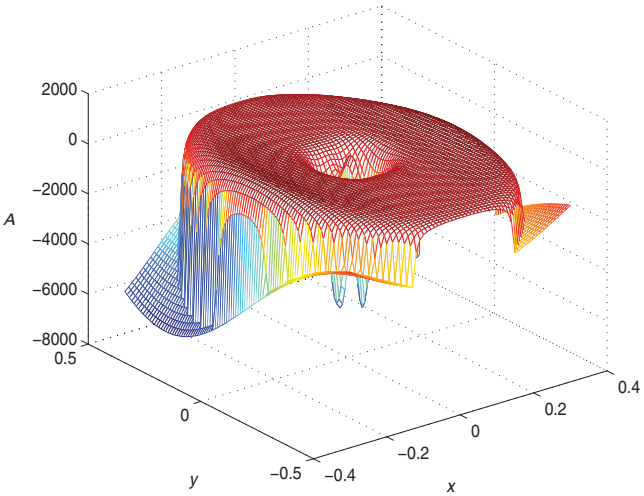

Figure 13. (Colour online) Stability function for the solution of Equilibrium 2. For most part of the equilibrium it is positive and assumes negative values only in the core of the equilibrium.

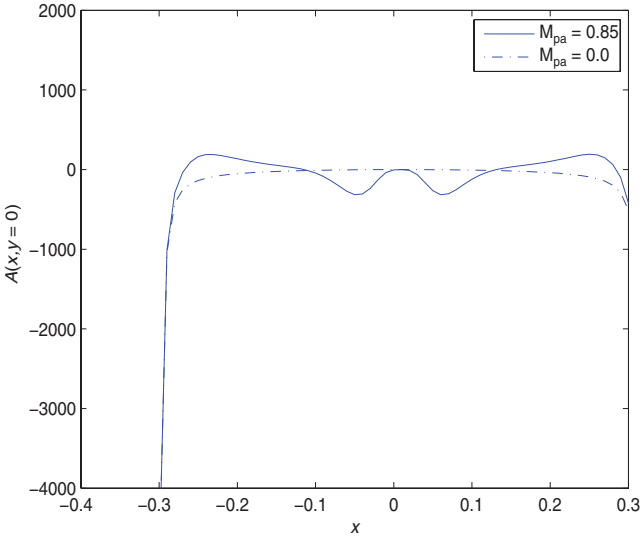

Figure 14. (Colour online) Plot of the stability function A, at $y = 0$, for the second equilibrium for non-zero values of the nonlinearity parameters $c3 = -3.099$ and $c4 = 1.033$. Increasing the flow parameter M_{pa} appears to improve stability for most part on the middle-plane except for the center of the equilibrium.

6. Summary

Two classes of solutions of nonlinear two-dimensional magnetohydrodynamic equilibria for bounded magnetically confined plasmas with sheared incompressible non-parallel flows have been constructed in cylindrical (z-independent) geometry. The equilibria hold for four arbitrary surface functions which were chosen to be the plasma density, axial Mach function, poloidal Mach function and static pressure.

After assigning the free functions, a systematic examination of equilibrium quantities and confinement figures of merit, as the safety factor, electric field and

https://doi.org/10.1017/S0022377812000918 Published online by Cambridge University Press

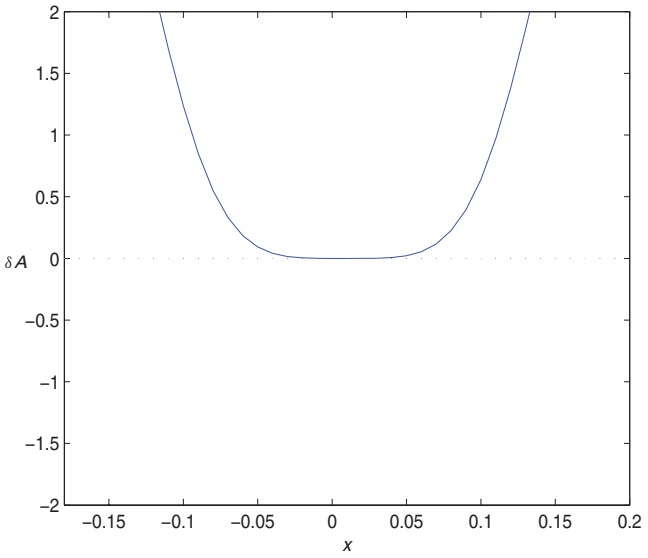

Figure 15. (Colour online) Plot of the deference $\delta A = A(n = 2) - A(n = 1)$ for $c3 = -3.099$, $c4 = 1.033$ and $M_{pa} = 0.1$ clearly indicating that the stability is improved ($\delta A > 0$) at the external part of the middle-plane $y = 0$ as the flow-shear parameter n increases. The dotted line represents the x-axis.

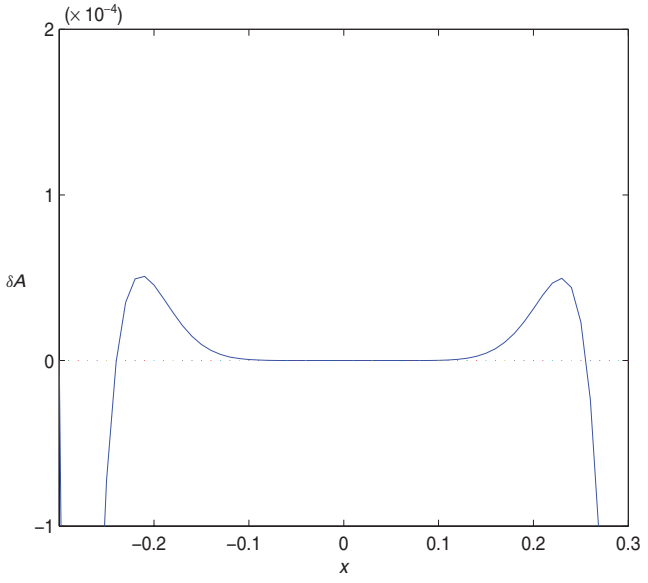

Figure 16. (Colour online) Plot of the profile $\delta A = A(c_3 = -3.099, c_4 = 1.033) - A(c_3 = c_4 = 0)$ at $y = 0$ indicating that the nonlinearity has a stabilizing effect ($\delta A > 0$) in the edge region.

$\mathbf{E} \times \mathbf{B}$ velocity shear for a variety of parametric values, implies that the equilibrium characteristics are qualitatively consistent with experimental evidence of the L–H transition. In addition, application of a sufficient condition for linear stability and parallel flow indicates that one stationary equilibrium being potential stable may describe the H state and another static equilibrium not satisfying the stability condition the L state. In addition, the equilibrium nonlinearity in conjunction with the flow and the flow shear may play a stabilizing role. Although understanding the physics of the L–H transition remains incomplete, the results of the present study may shed some light toward that goal.

Finally, it would be interesting trying to generalize these classes of solutions to up-down asymmetric configuration with a lower x-point in connection with the International Thermonuclear Experimental Reactor (ITER) project by potentially extending the ansatz (6) to include odd in y terms. Also, the study could be extended to toroidal geometry in order to examine the impact of toroidicity.

Acknowledgments

G.N.T. thanks Drs Henri Tasso and Calin Atanasiu for very useful discussions.

The work leading to this paper was performed within the participation of the University of Ioannina in the Association Euratom-Hellenic Republic, which is supported in part by the European Union (Contract of Association No. ERB 5005 CT 99 0100) and by the General Secretariat of Research and Technology of Greece. The views and opinions expressed herein do not necessarily reflect those of the European Commission.

References

Apostolaki, D., Throumoulopoulos, G. N. and Tasso, H. 2008 In: *35th EPS Conference on Plasma Phys. Hersonissos*, 9–13 June, ECA Vol. 32 (ed. P. Lalousis and S. Moustaizis). European Physical Society, p. 2.057.

Atanasiu, C. V., Gunter, S., Lackner, K. and Miron, I. G. 2004 *Phys. Plasmas* **11**, 3510.

Berk, H. L., Hammer, J. H. and Weitzner, H. 1981 *Phys. Fluids* **24**, 1758.

Betti, R. and Freidberg, J. P. 2000 *Phys. Plasmas* **7**, 2439.

Cerfon, A. J. and Freidberg, J. P. 2010 *Phys. Plasmas* **17**, 032502.

Clemente, R. A. and Farengo, R. 1984 *Phys. Fluids* **27**, 776.

de Vries, P. C., Joffrin, E., Brix, M., Challis, C. D., Crombé, K., Esposito, B., Hawkes, N. C., Giroud, C., Hobirk, J., Lönnroth, J., et al. 2009 *Nucl. Fusion* **49**, 075007.

Friedlander, S. and Vishik, M. M. 1995 *Chaos* **5**, 416.

Garcia, J. and Giruzzi, G. 2010 *Phys. Rev. Lett.* **104**, 205003.

Goedbloed, J. P. and Lifschitz, A. 1997 *Phys. Plasmas* **4**, 3544.

Grad, H. and Rubin, H. 1958 In: *Proceedings of the Second United Nations Conference on the Peaceful Uses of Atomic Energy*, Vol. 21. Geneva: United Nations, p. 190.

Greene, J. M. 1988 *Plasma Phys. Control. Fusion* **30**, 327.

Herrnegger, F. 1972 In: *Proceedings of the Fifth European Conference on Controlled Fusion and Plasma Physics*, Vol. I (ed Petit-Lancy). European Physical Society, p. 26.

Ilgisonis, V. I. and Pozdnyakov, Yu. I. 2004 *Plasma Phys. Rep.* **30**, 988.

Khater, A. H. and Moawad, S. M. 2009 *Phys. Plasmas* **16**, 122506.

Krasheninnikov, S. I., Soboleva, T. K. and Catto, P. J. 2002 *Phys. Lett.* A **298**, 171.

Kuiroukidis, Ap 2010 *Plasma Phys. Control. Fusion* **52**, 015002.

Kuiroukidis, Ap and Throumoulopoulos, G. N. 2011 *Plasma Phys. Control. Fusion* **53**, 125005.

Kuiroukidis, Ap and Throumoulopoulos, G. N. 2012 *Phys. Plasmas* **19**, 022508.

Malfliet, W. 2004 *J. Comput. Appl. Math.* **164–165**, 529.

Maschke, E. K. 1972 *Plasma Phys.* **15**, 535.

Mashke, E. K. and Perrin, H. 1984 *Phys. Lett.* A **102**, 106.

Mc Carthy, P. J. 1999 *Phys. Plasmas* **6**, 3554.

Mukhopadhyay, S. 2000 *Bull. Am. Phys. Soc.* **45**, 364.

Poulipoulis, G., Throumoulopoulos, G. N. and Tasso, H. 2005 *Phys. Plasmas* **12**, 042112.

Shafer, M. W., McKee, G. R., Austin, M. E. Burrell, K. H., Fonck, R. J. and Schlossberg, D. J. 2009 *Phys. Rev. Lett.* **103**, 075004.

Shafranov, V. D. 1958 *Sov. Phys. JETP* **6**, 545; (1957) *Zh. Eksp. Teor. Fiz.* **33**, 710.

Shi, B. 2011 *Nucl. Fusion* **51**, 023004.

Simintzis, Ch., Throumoulopoulos, G. N., Pantis, G. and Tasso, H. 2001 *Phys. Plasmas* **8**, 2641.

Solano, E. R. 2004 *Plasma Phys. Control. Fusion* **46**, L7.

Solovév, L. S. 1968 *Sov. Phys. JETP* **26**, 400; 1976 *Zh. Eksp. Teor. Fiz.* **53**, 626.

Srinivasan, R., Lao, L. L. and Chu, M. S. 2010 *Plasma Phys. Control. Fusion* **52**, 035007.

Tasso, H. and Throumoulopoulos, G. N. 1998 *Phys. Plasmas* **5**, 2378.

Tasso, H. and Throumoulopoulos, G. N. 2012 *J. Plasma Physics* **78**, 1.

Terry, P. W. 2000 *Rev. Mod. Phys.* **72**, 109.

Throumoulopoulos, G. N. and Pantis, G. 1996 *Plasma Phys. Control. Fusion* **38**, 1817.

Throumoulopoulos, G. N. and Tasso, H. 1997 *Phys. Plasmas* **4**, 1492.

Throumoulopoulos, G. N. and Tasso, H. 2007 *Phys. Plasmas* **14**, 122104.

Throumoulopoulos, G. N. and Tasso, H. 2010 *Phys. Plasmas* **17**, 032508.

Throumoulopoulos, G. N. and Tasso, H. 2012 *Phys. Plasmas* **19**, 014504.

Throumoulopoulos, G. N., Weitzner, H. and Tasso, H. 2006 *Phys. Plasmas* **13**, 122501.

Throumoulopoulos, G. N., Tasso, H. and Poulipoulis, G. 2008 *J. Plasma Physics* **74**, 327.

Throumoulopoulos, G. N., Tasso, H. and Poulipoulis, G. 2009 *J. Phys. A: Math. Theor.* **42**, 335501.

Tsui, K. H. and Navia, C. E. 2012 *Phys. Plasmas* **19**, 012505.

Tsui, K. H., Navia, C. E., Serbeto, A. and Shigueoka, H. 2011 *Phys. Plasmas* **18**, 072502.

Vladimirov, V. A. and Ilin, K. I. 1998 *Phys. Plasmas* **5**, 4199.

Weening, R. H. 2000 *Phys. Plasmas* **7**, 3654.

Yavorskij, V. A., Schoepf, K., Andrushchenko, Zh. N., Cho, B. H., Goloborod'ko, V. Ya. and Reznyk, S. N. 2001 *Plasma Phys. Control. Fusion* **43**, 249.